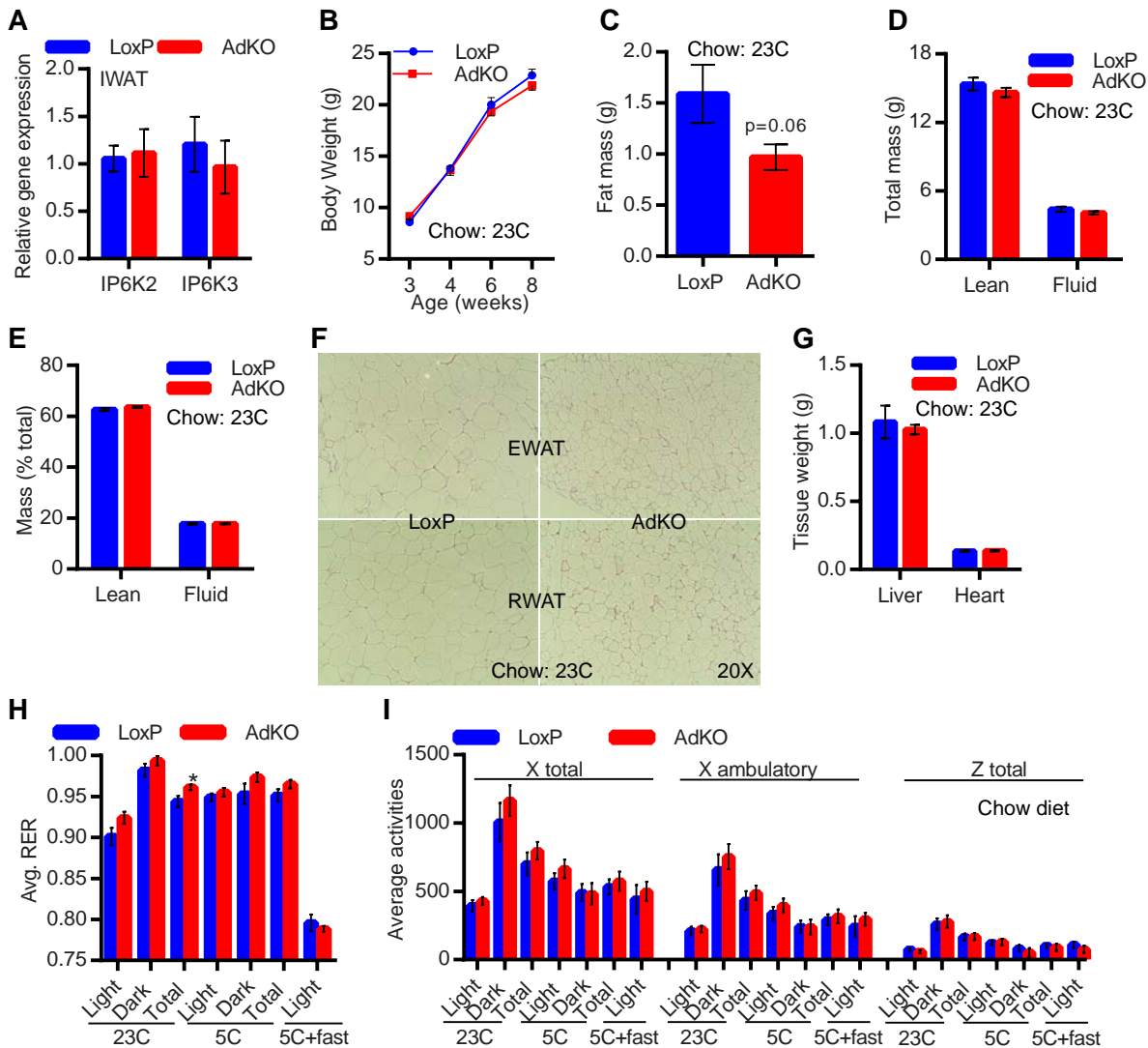
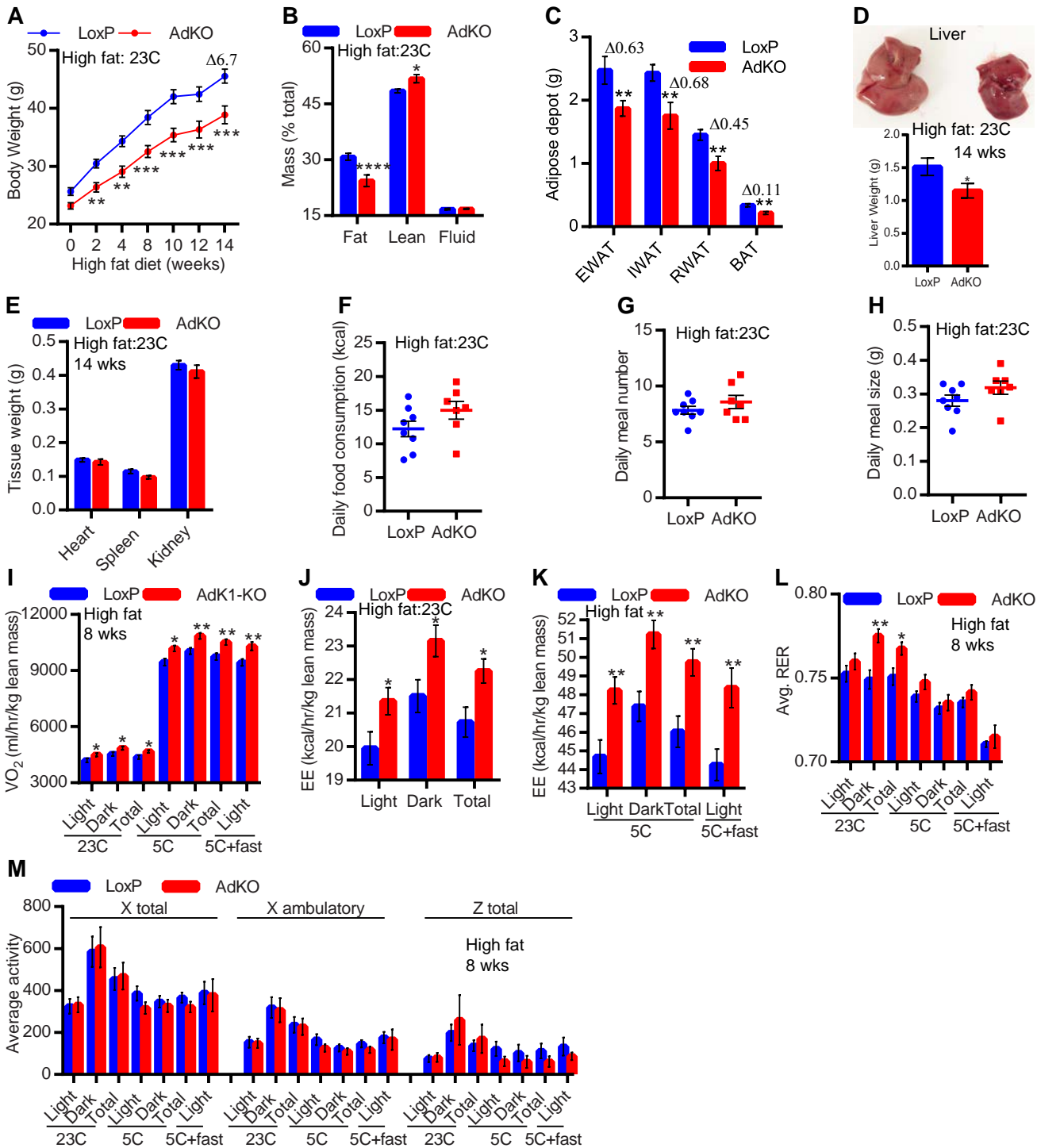


Supplemental Figure 1: Adipocyte-specific *IP6K1* deleted mice accumulate less fat due to enhanced thermogenic EE under chow-fed conditions



**Supplemental Figure 1: Adipocyte-specific *IP6K1* deleted mice accumulate less fat due to enhanced thermogenic EE under chow-fed conditions.** **A.** *IP6K2* or *IP6K3* does not compensate for *IP6K1* in the adipose tissue of AdKO mice (n=8 mice/group; t-test). **B.** Chow-fed AdKO mice exhibit similar body weight as their LoxP littermates (n=15 mice/group; Two-Way Anova). **C.** Chow-fed AdKO mice display a slight reduction in total fat mass (n=10 mice/group; t-test). **D and E.** Total and percent lean and fluid masses are unaltered in chow-fed AdKOs (n=10 mice/group; t-test). **F.** Adipocyte size is slightly smaller in chow-fed AdKO mice. Histology images represent results obtained from n=3 mice/group. **G.** Liver and heart weights are similar in LoxP and AdKO mice (n=4/group; t-test). **H.** Average RER is slightly higher in chow-fed AdKO mice at 23°C (n=8/group; t-test). **I.** Average activity profiles are similar in chow-fed AdKO and LoxP mice (n=8/group; t-test). Data in all panels expressed as mean  $\pm$ SEM. \*P<0.05.

Supplemental Figure 2: Increased thermogenic EE decelerates HFD-induced weight gain in AdKO mice

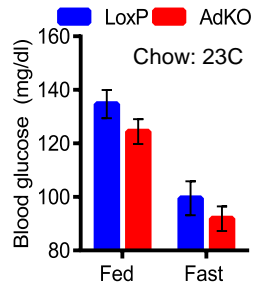


**Supplemental Figure 2: Increased thermogenic EE decelerates HFD-induced**

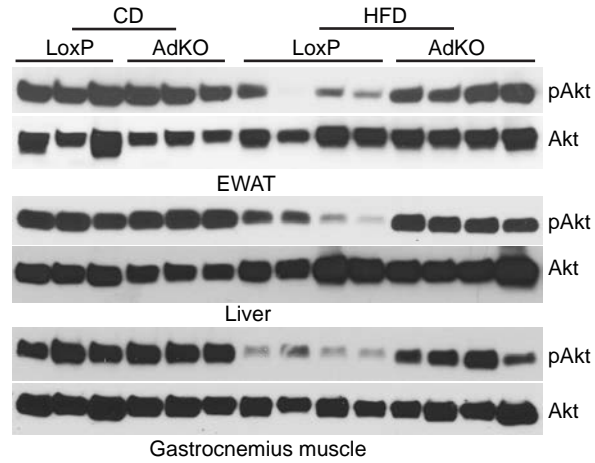
**weight gain in AdKO mice. A.** At 23°C, AdKO mice display less total body weight when exposed to a HFD (n=15 mice/group; Two-Way Anova). **B.** Percent fat mass (over total body weight) is significantly less whereas percent lean mass is slightly higher in HFD-AdKOs. Percent fluid mass is unaltered (n=10 mice/group; t-test). **C.** Weight of diverse adipose tissue depots are less in HFD-AdKOs (n=10 mice/group; t-test). **D.** Upper panel: Liver of HFD-fed AdKO mice appears smaller and healthier. Liver photograph represents images from n=10 mice/group. Lower panel: Liver weight is less in HFD-fed AdKO mice (n=10 mice/group; t-test). **E.** Weights of heart, spleen and kidney are largely similar in HFD-fed AdKO mice at 23°C (n=10 mice/group; t-test). **F.** Average daily food intake is slightly albeit insignificantly higher in HFD-fed AdKO mice (14.98 kcals) compared to their LoxP littermates (12.23 kcals) (n=7-8 mice/group; t-test). **G and H.** Daily meal size and meal number are largely similar in HFD-AdKOs and LoxPs at 23°C (n=7-8 mice/group; t-test). **I.** Average VO<sub>2</sub> consumption is higher in HFD-AdKO at 23°C and 5°C (n=8 mice/group; t-test). **J and K.** Higher EE in HFD-AdKO at 23°C and 5°C (n=8 mice/group; t-test). **L.** RER is slightly higher in HFD-AdKO at 23°C but it is similar at 5°C (n=8 mice/group; t-test). **M.** Average activity profiles are unchanged in HFD-fed AdKO mice at 23°C and 5°C (n=8 mice/group; t-test). Data in all panels expressed as mean ±SEM. \*P<0.05, \*\*P<0.01, \*\*\*P<0.001.

Supplemental Figure 3: Adipocyte-specific *IP6K1* deletion protects mice from HFD-induced insulin resistance

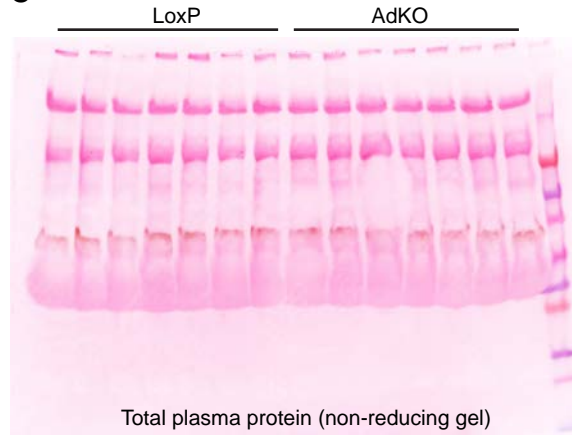
**A**



**B**

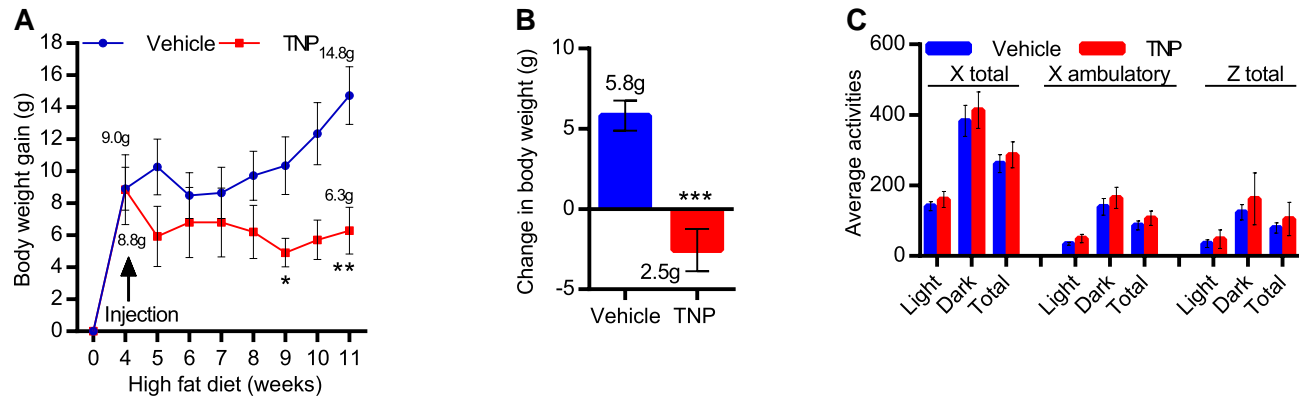


**C**



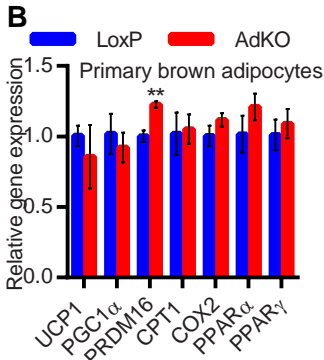
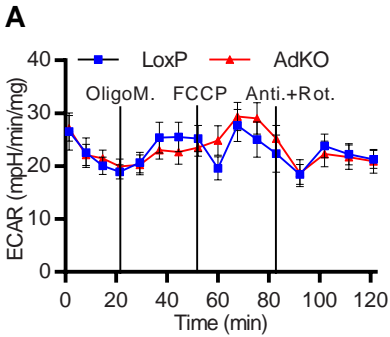
**Supplemental Figure 3: Adipocyte-specific *IP6K1* deletion protects mice from HFD-induced insulin resistance.** **A.** Blood glucose level is marginally lower in CD-fed AdKO mice (n=10-13 mice/group; t-test). **B.** Akt stimulatory phosphorylation is similar in various metabolic tissues of CD-fed LoxP and AdKO mice. HFD-feeding reduces Akt phosphorylation in LoxP mice to a higher extent whereas AdKO mice are largely protected. Therefore, enhanced Akt phosphorylation is observed in HFD-fed AdKO compared to their LoxP littermates (n=3-4 mice/group). **C.** Ponceau staining for loading of plasma samples in the experiment described in Figure 3H (n=7 mice/group).

Supplemental Figure 4: Pharmacologic inhibition of IP6K enhances thermogenic EE and blocks the progression of HFD-induced obesity



**Supplemental Figure 4: Pharmacologic inhibition of IP6K enhances thermogenic EE and blocks the progression of HFD-induced obesity.** **A.** After 4 weeks of HFD-feeding, mice gained an average body weight of 8.9g. At this point, injection was started (arrow). After 7 weeks of injection in HFD-fed mice, vehicle group gained an average of 14.8g body weight. Conversely, TNP treated mice gained only 6.3g (n=5 mice/group; Two-Way Anova). **B.** During 7 weeks of injection, vehicle mice gained an average of 5.8g whereas TNP-mice lost 2.5g body weight (n=5 mice/group; t-test). **C.** Average activity profiles are similar in vehicle and TNP treated mice (n=5 mice/group; t-test). Data in all panels expressed as mean  $\pm$ SEM. \*P<0.05, \*\*P<0.01, \*\*\*P<0.001.

Supplemental Figure 5: Adipocyte-specific *IP6K1* deletion enhances browning

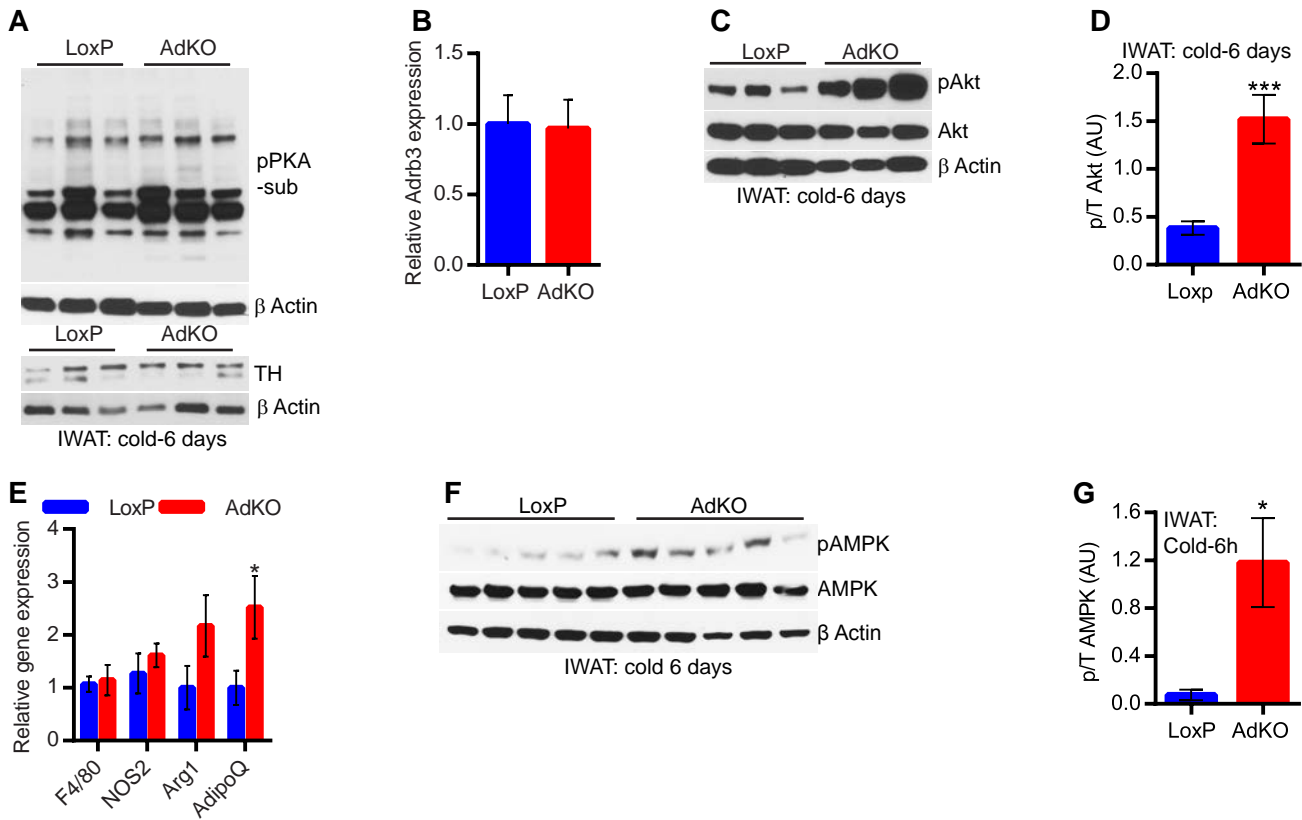


**Supplemental Figure 5: Adipocyte-specific *IP6K1* deletion enhances browning.** **A.**

Extracellular acidification rate (ECAR) is similar in LoxP and AdKO-IWAT beige adipocytes which indicates similar rate of glycolysis in two genotypes (n=6 mice/preparation; 10 replicates). **B.** SVFs (n=6 mice/group) isolated from BAT of LoxP and AdKO mice when differentiated in vitro, display similar levels of browning and mitochondrial marker expression (triplicate samples). Data expressed as mean  $\pm$ SEM.

\*\*P<0.01.

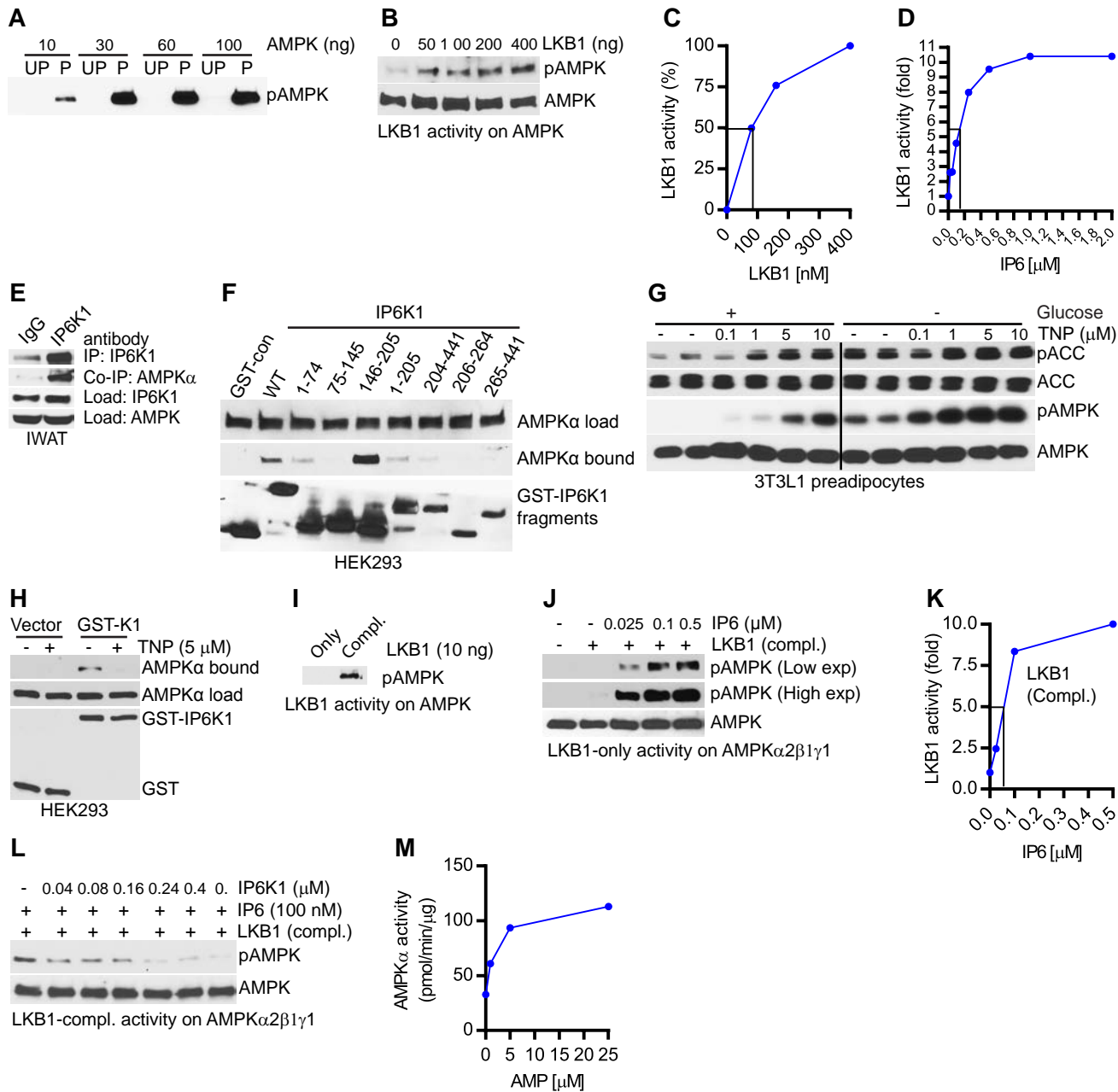
Supplemental Figure 6: IP6K1 reduces AMPK mediated adipocyte browning



**Supplemental Figure 6: IP6K1 reduces AMPK mediated adipocyte browning. A.**

Upper panel: Global PKA activity is unaltered in chronic cold-exposed AdKO mice. Lower panel: Tyrosine hydroxylase (TH) protein level is also similar LoxP and AdKO IWAT (n=3 mice/group). **B.** *Adrb3* expression is unaltered in chronic cold-exposed AdKO mice (n=8 mice/group). **C and D.** Akt stimulatory phosphorylation is 3-fold higher in chronic cold-exposed AdKO mice (n=3 mice/group; t-test). **E.** Chronic cold exposure induces AdipoQ mRNA expression level to a higher extent in AdKO-IWAT. However, the general macrophage marker F4/80, M1-specific NOS2 and M2-specific Arg1 are unaltered under these conditions (n=8 mice/group; t-test). **F.** AMPK activity is slightly higher in chronic cold exposed AdKO mice (n=5 mice/group). **G.** Densitometry of Figure 6B reveals that AMPK stimulatory phosphorylation is ~5 fold higher in AdKO compared to LoxP mice following acute cold-exposure (n=3 mice/group; t-test). Data in all panels expressed as mean  $\pm$ SEM. \*P<0.05, \*\*\*P<0.001.

Supplemental Figure 7: IP6 and IP6K1 differentially regulate AMPK stimulatory phosphorylation

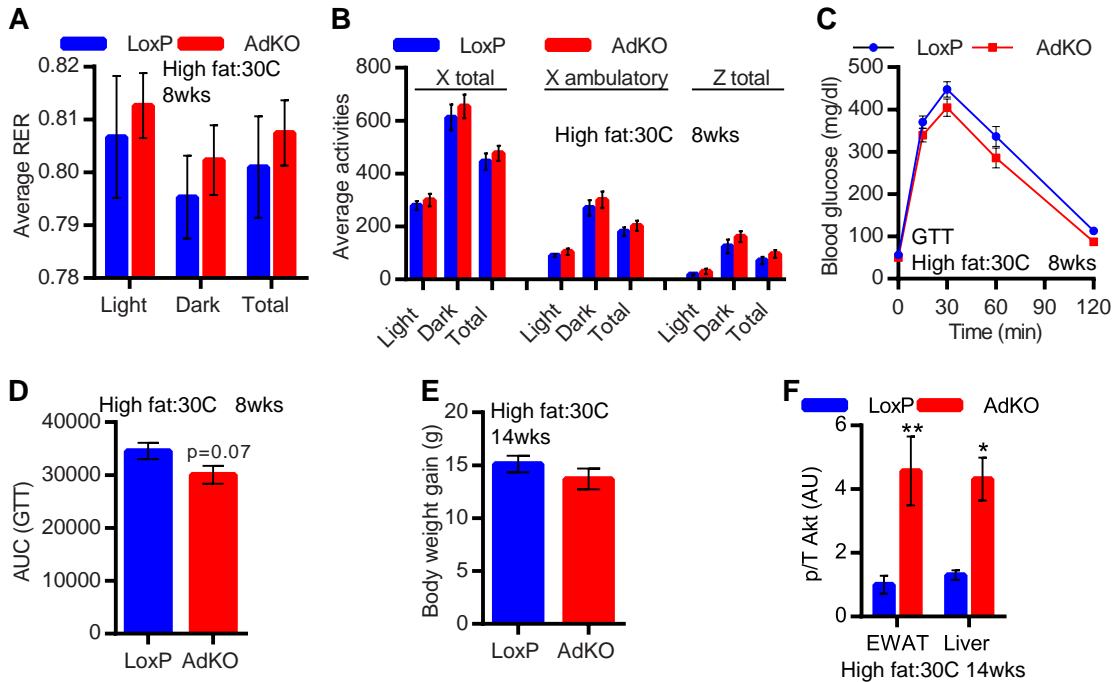


**Supplemental Figure 7: IP6 and IP6K1 differentially regulate AMPK stimulatory**

**phosphorylation. A.** Inactive AMPK complex (AMPK $\alpha$ 2 $\beta$ 1 $\gamma$ 1) does not display AMPK $\alpha$  (T172) phosphorylation (UP: unphosphorylated) whereas the active version does (P: phosphorylated). The inactive version was used as a LKB1 substrate in the assay. Data represent results obtained from three independent experiments. **B and C.** LKB1-only (without its co-activator proteins MO25 and STRAD $\alpha$ ) phosphorylates inactive AMPK $\alpha$ 2 $\beta$ 1 $\gamma$ 1. Data represent results obtained from three independent experiments. **D.** Quantification of Figure 7B reveals that IP6 (EC<sub>50</sub> ~150 nM) enhances LKB1-only mediated AMPK  $\alpha$ 2 $\beta$ 1 $\gamma$ 1 phosphorylation. Data represent results obtained from three independent experiments. **E.** Endogenous IP6K1 and AMPK interact in the IWAT depot. Data represent results obtained from two independent experiments. **F.** Deletion mapping reveals that residues 146-205 of human IP6K1 interact with endogenous AMPK $\alpha$ . GST and various mutants of GST-IP6K1 were overexpressed in HEK293 cells. **G.** TNP, at increasing concentrations, enhances AMPK phosphorylation and activity in 3T3L1 preadipocytes under basal and glucose deprived conditions. Data represent results from at least three independent experiments. **H.** TNP disrupts GST-IP6K1's interaction with endogenous AMPK $\alpha$  in HEK293 cells. Data represent results from three independent experiments. **I.** LKB1-complex (10 ng/reaction), efficiently phosphorylates AMPK  $\alpha$ 2 $\beta$ 1 $\gamma$ 1. At this concentration, LKB1-only is ineffective. Data represent results obtained from three independent experiments. **J and K.** IP6 efficiently (EC<sub>50</sub> ~80 nM) stimulates LKB1-complex (with MO25 and STRAD $\alpha$ ) mediated AMPK phosphorylation. Data represent results from three independent experiments. **L.** IP6K1 inhibits IP6 mediated stimulation of AMPK phosphorylation by the LKB1-complex. Data represent results obtained from

three independent experiments. **M.** AMP, at reported concentrations, stimulates AMPK activity on SAMSTIDE in vitro. Data represent results from three independent experiments.

Supplemental Figure 8: Thermoneutrally placed HFD-AdKO mice do not display leanness albeit exhibit insulin sensitivity



**Supplemental Figure 8: Thermoneutrally placed HFD-AdKO mice do not display leanness albeit exhibit insulin sensitivity.** **A.** Average RER is unaltered in AdKO mice after 8-weeks of HFD at 30°C (n=6 mice/group; t-test). **B.** Average activity profiles are similar in AdKO-30°C and LoxP (n=6 mice/group; t-test). **C and D.** AdKO mice dispose glucose at a slightly (not significant) higher rate than LoxPs after 8 weeks of HFD, at 30°C (n=6 mice/group; Two-Way Anova and t-test for Supplemental Figures 8C and 8D respectively). **E.** After 14 weeks of HFD at 30°C, average body weights of LoxP and AdKO mice are similar (n=6 mice/group; t-test). **F.** Densitometry of Figure 8H reveals that AdKO mice, after 14 weeks of HFD-feeding at 30°C, display ~4-fold enhancements in Akt stimulatory phosphorylation in EWAT and liver (n=4 mice/group; t-test). Data in all panels expressed as mean ±SEM. \*P<0.05, \*\*P<0.01.

Blots: Related to Figure 1

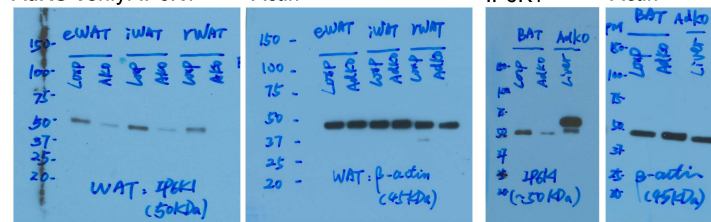
### Figure 1B

AdKO verify: IP6K1

Actin

IP6K1

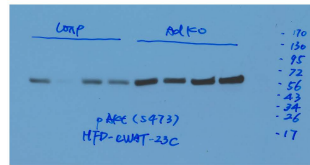
Actin



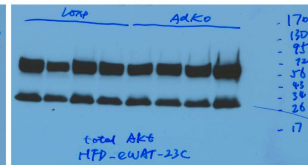
Blots: Related to Figure 3

Figure 3F

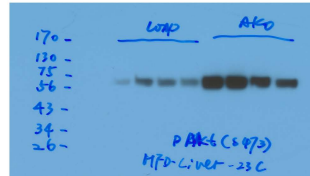
AdKO HFD eWAT: pAkt



AdKO HFD eWAT: tAkt



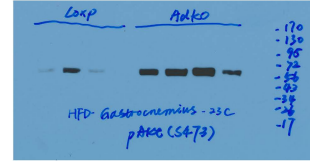
AdKO HFD Liver: pAkt



AdKO HFD Liver: tAkt



AdKO HFD Muscle: pAkt



AdKO HFD Muscle: tAkt

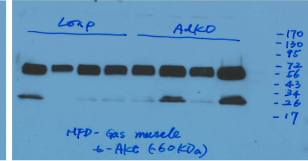
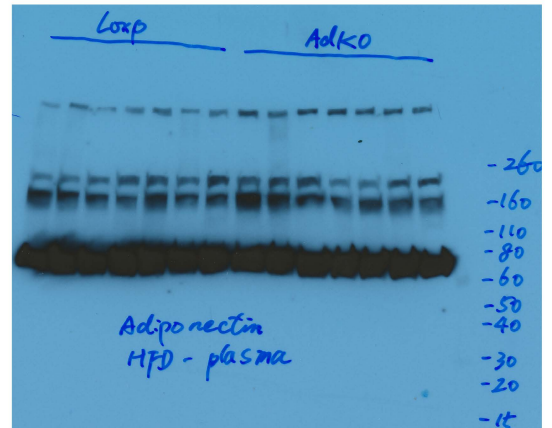
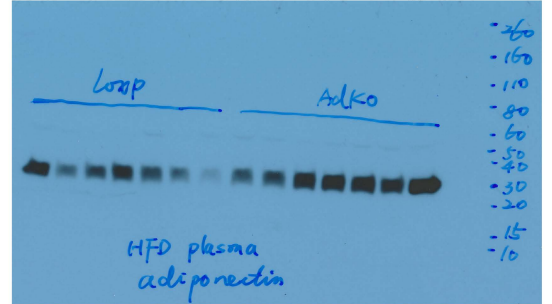


Figure 3H

AdKO HFD plasma: Adiponectin (Nonreducing)



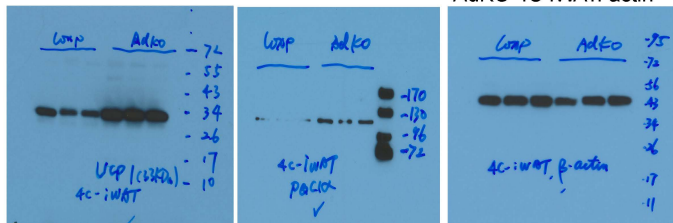
AdKO HFD plasma: Adiponectin (Reducing)



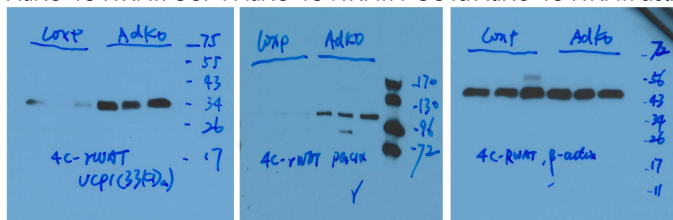
Blots: Related to Figure 5

### Figure 5C

AdKO 4C iWAT: UCP1    AdKO 4C iWAT: PGC1 $\alpha$     AdKO 4C iWAT: actin



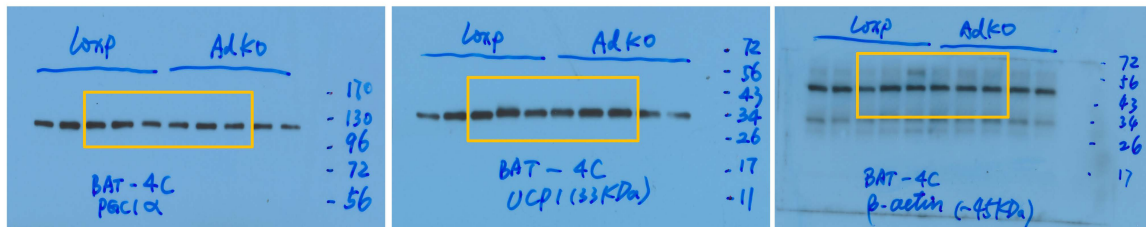
AdKO 4C RWAT: UCP1    AdKO 4C RWAT: PGC1 $\alpha$     AdKO 4C RWAT: actin



AdKO 4C-BAT: UCP1

AdKO 4C-BAT: PGC1 $\alpha$

AdKO 4C-BAT: actin

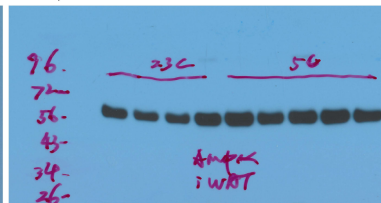
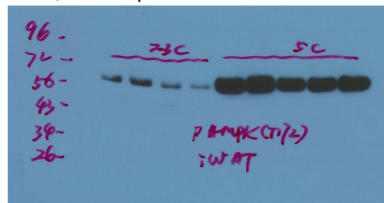


Blots: Related to Figure 6

**Figure 6A**

iWAT, 23-5C: pAMPK

iWAT, 23-5C: AMPK



iWAT, 23-5C: pACC

iWAT, 23-5C: ACC

iWAT, 23-5C: actin

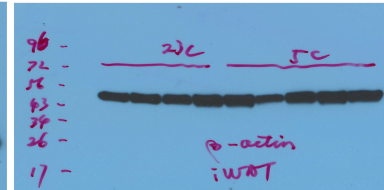
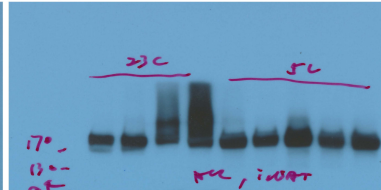
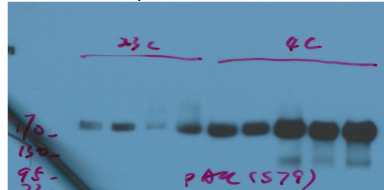


**Figure 6B**

iWAT-5C-6h: pAMPK

iWAT-5C-6h: AMPK

**Figure 6C**

Beige: pACC

Beige: ACC

Beige: pAMPK

Beige: AMPK

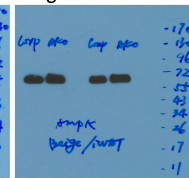
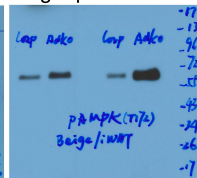
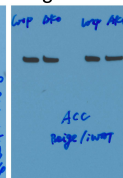
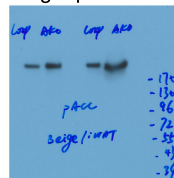
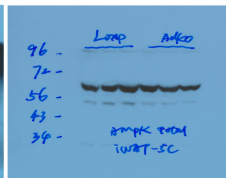
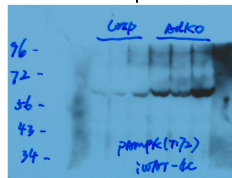


**Figure 6D**

Beige: AMPK

Beige: PGC1α

Beige: UCP1

Beige: actin

**Figure 6E**

TNP: pAMPK

TNP: AMPK

TNP: pACC

TNP: ACC

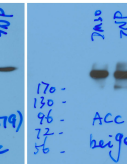
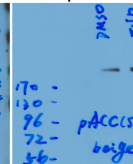
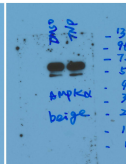
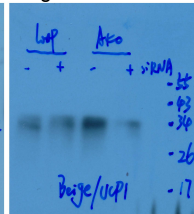
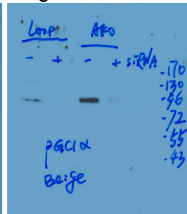
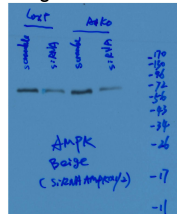


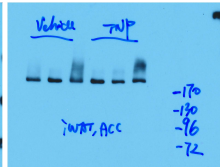
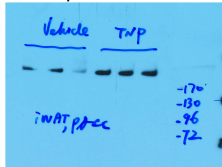
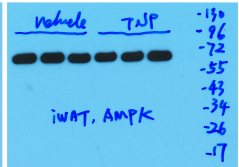
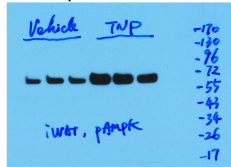
**Figure 6H**

iWAT: pAMPK

iWAT: AMPK

iWAT: pACC

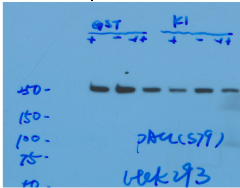
iWAT: ACC



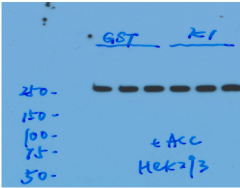
Blots: Related to Figure 7

**Figure 7A**

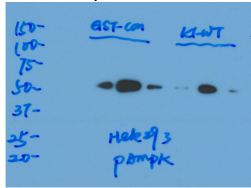
Hek293: pACC



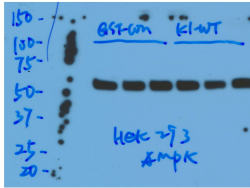
Hek293: ACC



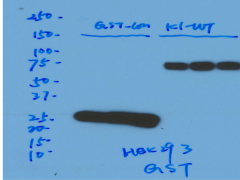
Hek293: pAMPK



Hek293: AMPK



Hek293: GST



Hek293: actin

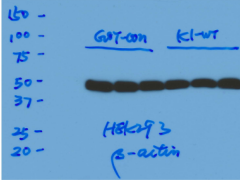
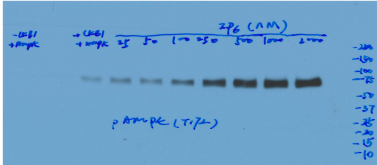


**Figure 7B**

IP6 doses: pAMPK



5-IP7 on AMPK: pAMPK

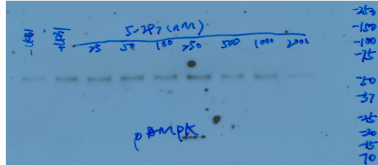
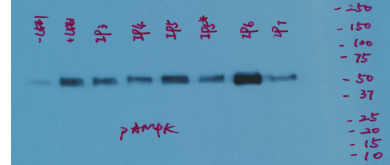
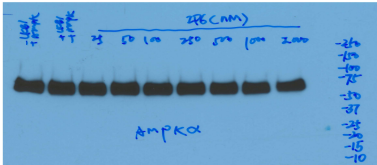


**Figure 7D**

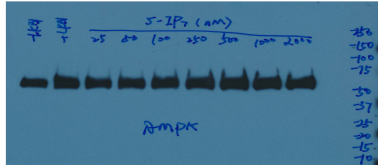
IPs on AMPK: pAMPK



IP6 doses: AMPK



5-IP7 on AMPK: AMPK



IPs on AMPK: AMPK

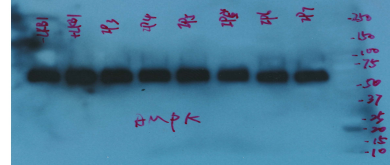
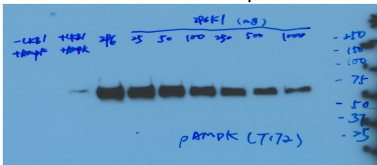


**Figure 7E**

WT-IP6K1 on IP6-AMPK: pAMPK



Inactive K1 on AMPK: pAMPK

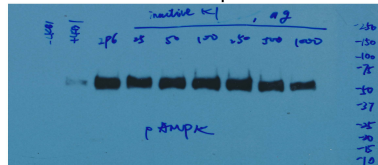
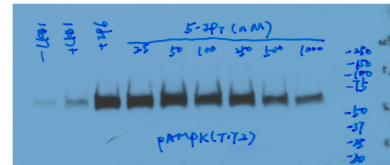
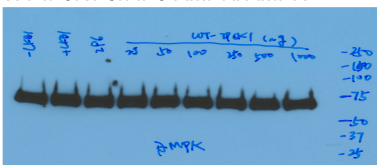


**Figure 7F**

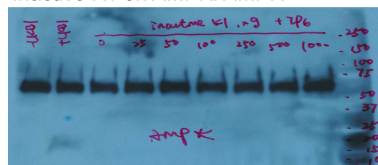
5-IP7 on IP6-AMPK: pAMPK



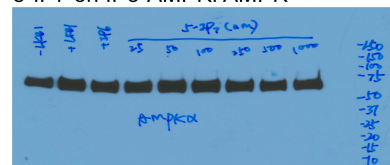
WT-IP6K1 on IP6-AMPK: AMPK



Inactive K1 on AMPK: AMPK



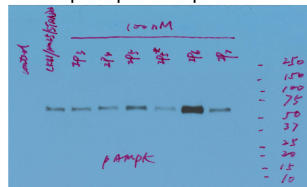
5-IP7 on IP6-AMPK: AMPK



Blots: Related to Figure 7

**Figure 7G**

Institol phosphates: pAMPK



Institol phosphates: AMPK

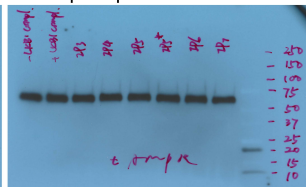
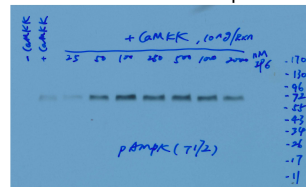


**Figure 7H**

IP6 on CaMKK-AMPK: pAMPK



IP6 on CaMKK-AMPK: AMPK

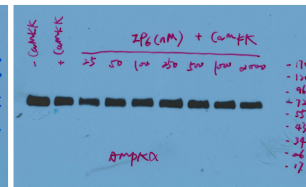
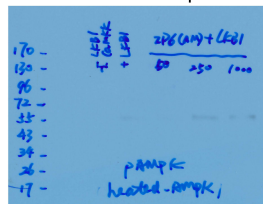


**Figure 7I**

Denatured-AMPK: pAMPK



Denatured-AMPK: AMPK

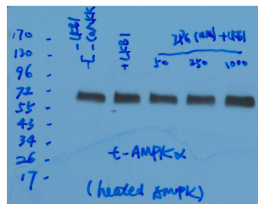


**Figure 7J**

IP6 on AMPKa2b1g1 or AMPKa2 only

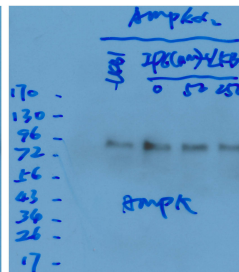
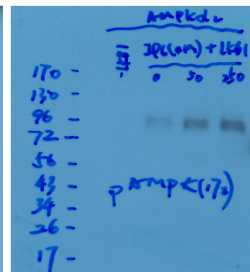
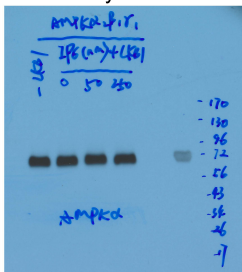
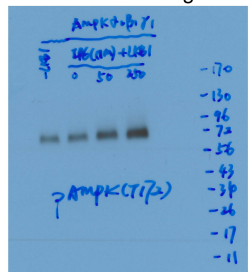
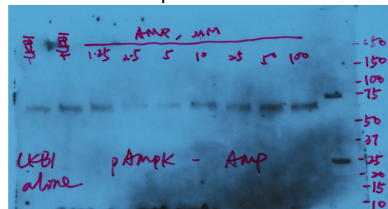
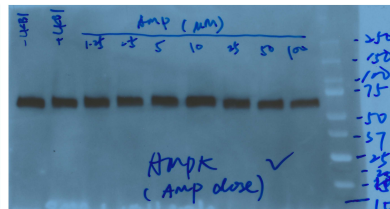


**Figure 7K**

AMP on AMPK: pAMPK



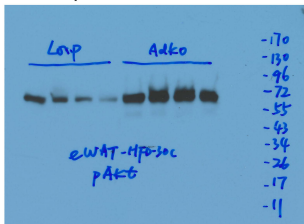
AMP on AMPK: AMPK



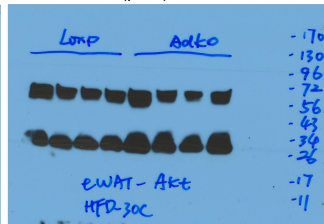
Blots: Related to Figure 8

Figure 8H

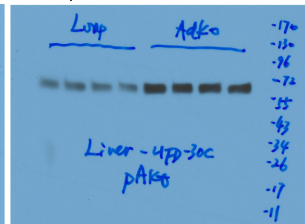
EWAT: pAkt



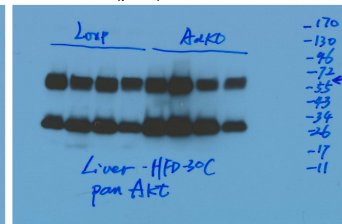
EWAT: tAkt (pan)



Liver: pAkt



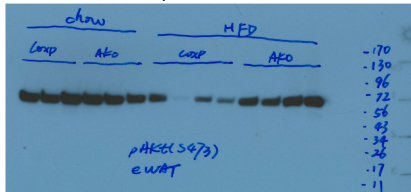
Liver: tAkt (pan)



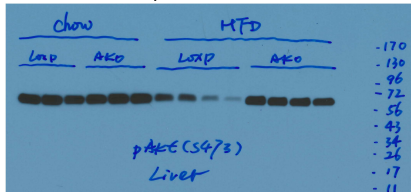
Blots: Related to Supplemental Figure 3

**Figure S3B**

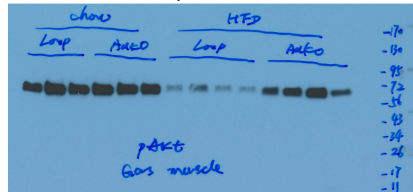
CD-HFD-EWAT: pAkt



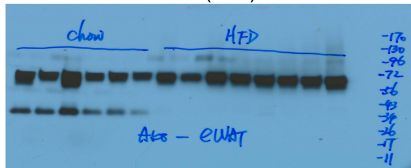
CD-HFD-Liver: pAkt



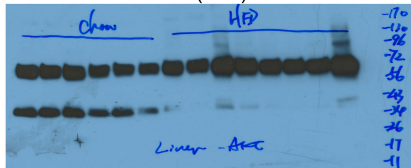
CD-HFD-Muscle: pAkt



CD-HFD-EWAT: tAkt (Pan)



CD-HFD-Liver: tAkt (Pan)



CD-HFD-Muscle: tAkt (Pan)

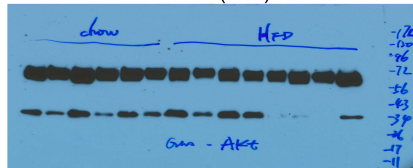


**Figure S3C**

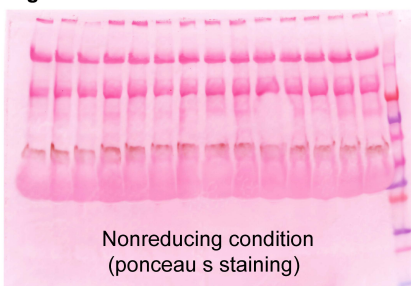


**Figure S6A**

AdKO 4C iWAT: pPKA-sub AdKO 4C iWAT: actin AdKO 4C iWAT: TH

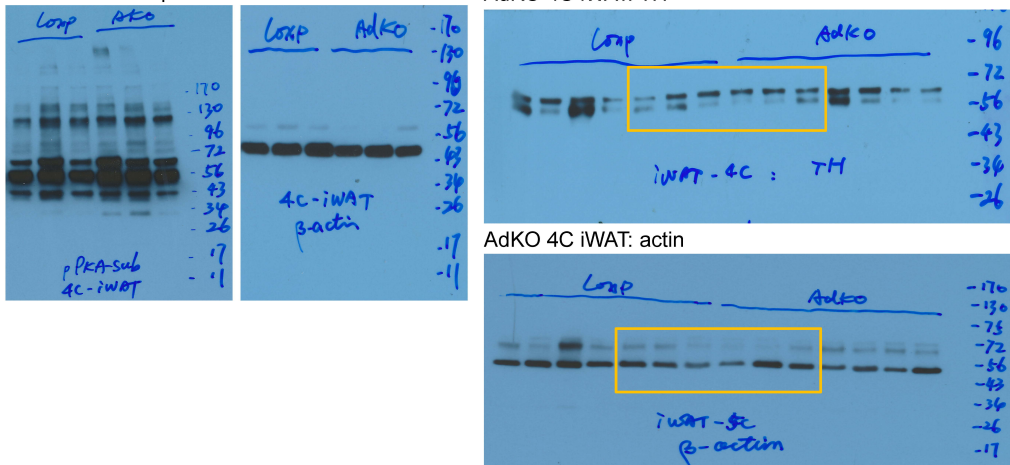


**Figure S6C**

AdKO-5C-iWAT: pAkt AdKO-5C-iWAT: Akt AdKO-5C-iWAT: actin

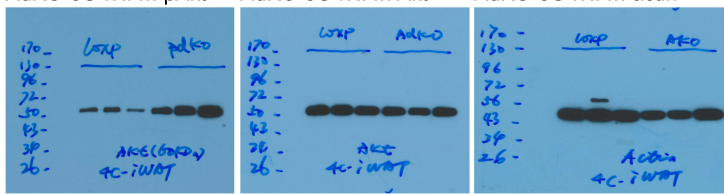


**Figure S6F**

AdKO-5C-iWAT: pAMPK AdKO-5C-iWAT: AMPK AdKO-5C-iWAT: actin

